Two Photon Absorption – Transient Current Technique

Results of TCAD Simulation of TPA-TCT in a pad detector
&
Influence of Radiation Damage on the TPA-TCT

Marcos Fernández García[1,2], Michael Moll[1], Sebastian Pape[1,3], Moritz Wiehe[1]

[1]CERN
[2]Instituto de Física de Cantabria
[3]TU Dortmund University

RD50 2002 - 2023

https://indico.cern.ch/event/1334364/

29.11.2023

43rd RD50 workshop – S. Pape
at CERN

E-mail: sebastian.pape@cern.ch

Table of content

Part I

Results of TCAD simulation of TPA-TCT in a pad detector

TCAD

Part II
Continuation of my 42nd RD50 talk

Comparison between neutron, proton, and gamma irradiated samples

Influence on the linear absorption coefficient and refractive index

Radiation damage and the TPA-TCT

Part I

Results of TCAD Simulation of TPA-TCT in a pad detector

See **Michael's talk** for details of the simulations!

TCAD simulation of TPA-TCT

Experiment

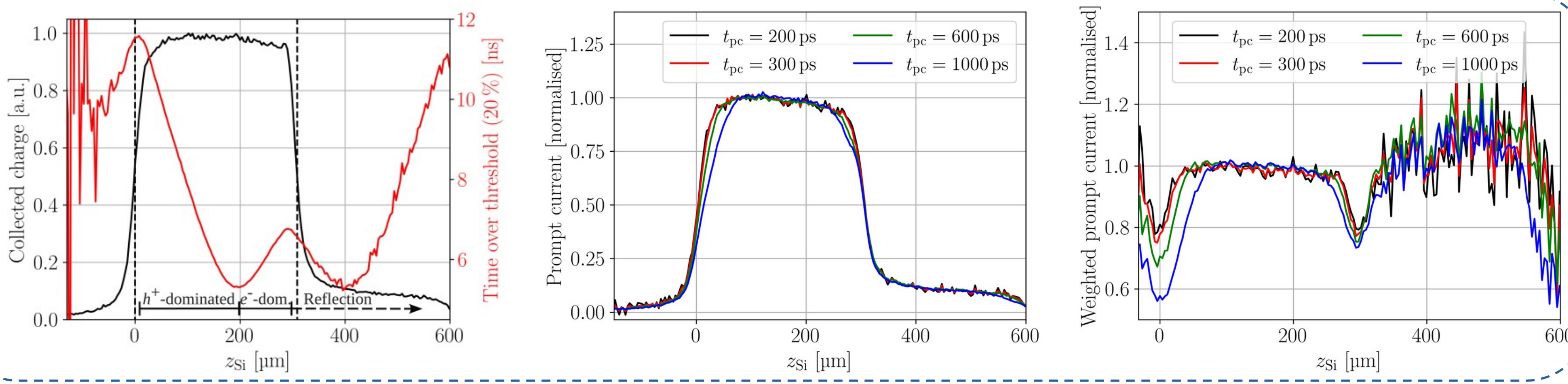

Simulation

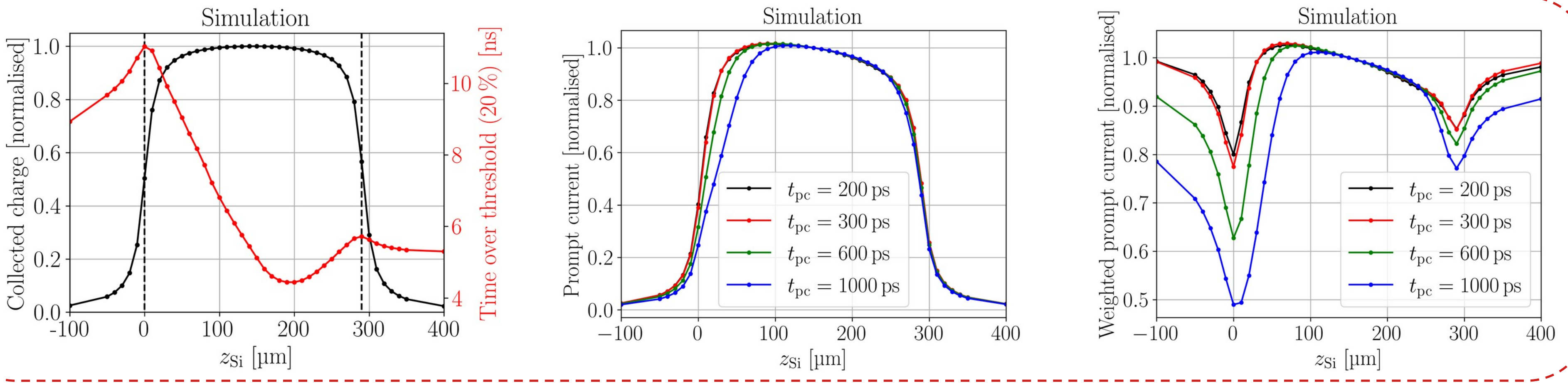

Plots from S. Pape Thesis (2024)

TCAD simulation of TPA-TCT: Definitions

Time over threshold (ToT):

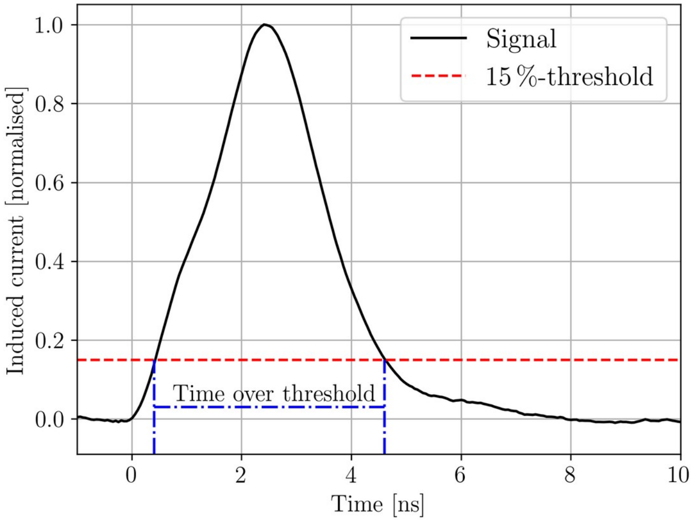

- The threshold is defined as a certain fraction of the amplitude
- Calculated individually for each waveform

Extraction of charge Q and prompt current (PC):

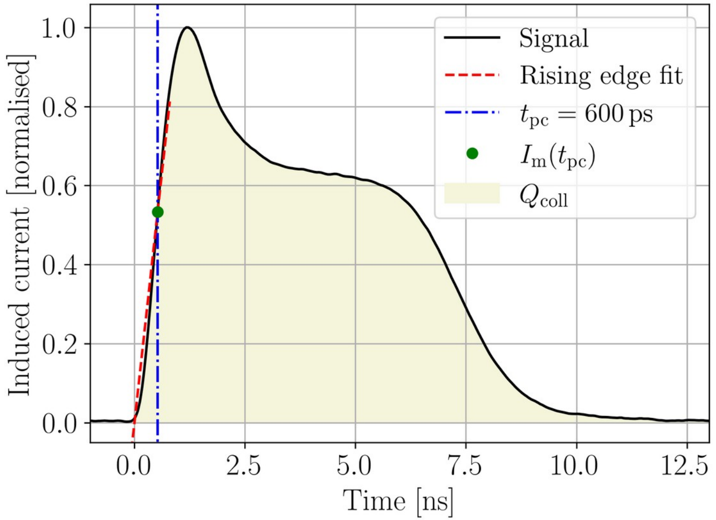

Plots from S. Pape Thesis (2024)

- Beginning of signal: found by fit to the rising edge
- PC: Current at a given time t_{pc} after the beginning
- Q_{coll}: Integral of the current transient until a given time t_{coll}

- Weighted prompt current: $I(t_{pc})$ / Q_{coll}

Details: https://doi.org/10.3390/s23020962

TCAD simulation of TPA-TCT: Time-over-threshold

Closer look on the ToT profile:

- Where do the maxima at the boundaries originate from?

  → Expectation: ToT is constant beyond the boundaries as charge is deposited at the maximum positions

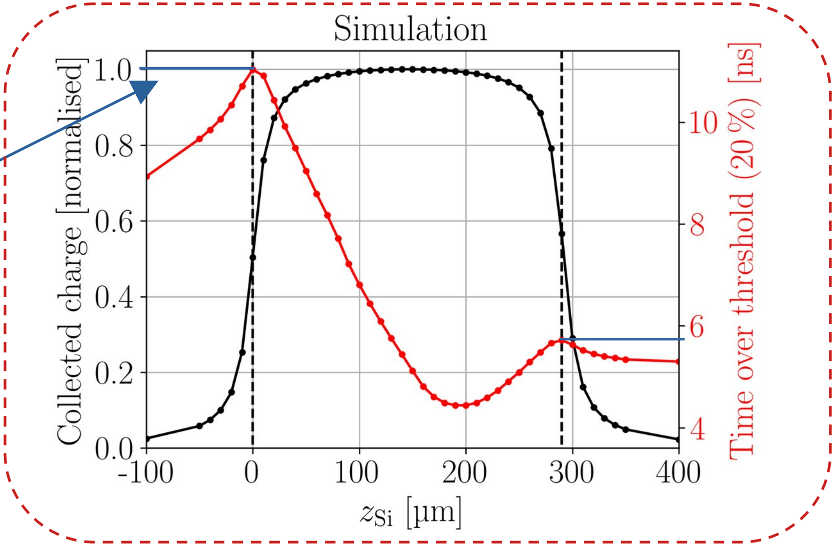

Plots from S. Pape Thesis (2024)

TCAD simulation of TPA-TCT: Time-over-threshold

Closer look on the ToT profile:

- Where do the maxima at the boundaries originate from?

→ Expectation: ToT is constant beyond the boundaries as charge is deposited at the maximum positions

→ The maxima originate from the assumption that the focal point positions aligns with the position of the dominant contribution to the current transient

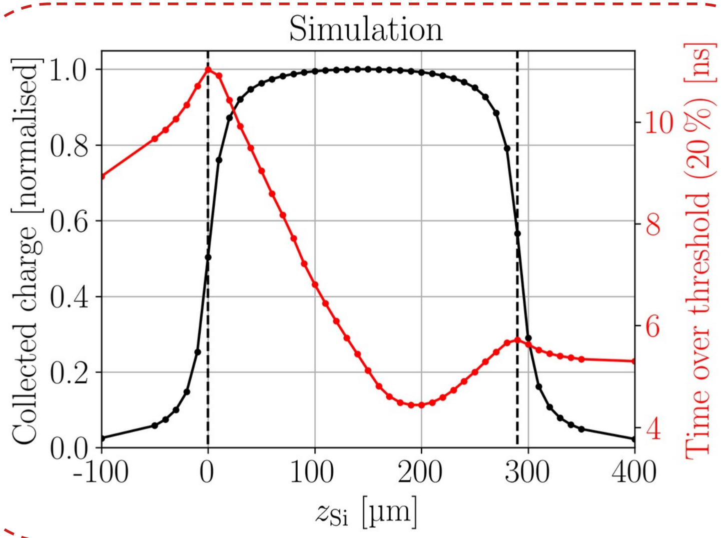

Plots from S. Pape Thesis (2024)

TPA charge carrier density along depth:

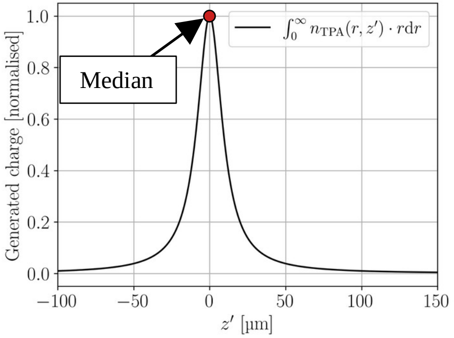

The median is central when the full distribution is inside the active volume.

Definition:
The median is the position of the main contribution to the charge generation.
It is calculated as the position where the integral of the excess charge carrier density reaches 50%.

TCAD simulation of TPA-TCT: Time-over-threshold

Closer look on the ToT profile:

- Where do the maxima at the boundaries originate from?

  → Expectation: ToT is constant beyond the boundaries as charge is deposited at the maximum positions

  → The maxima originate from the assumption that the focal point positions aligns with the position of the dominant contribution to the current transient

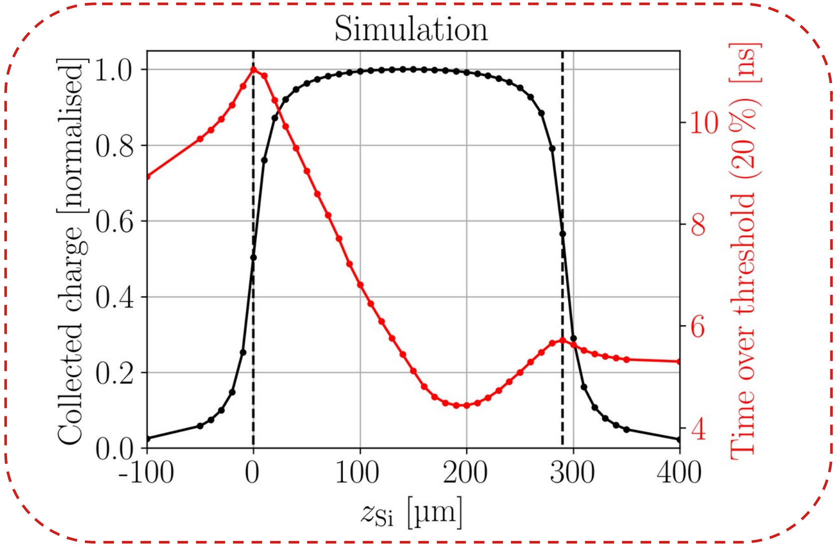

Plots from S. Pape Thesis (2024)

TPA charge carrier density along depth:

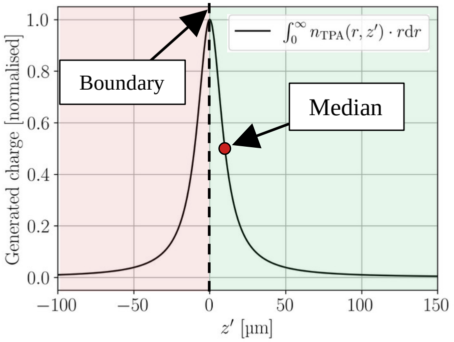

The median is central when the full distribution is inside the active volume, **but the median position shifts when one is close to the boundaries.**

This causes the ToT to become "symmetric" around the boundaries!

TCAD simulation of TPA-TCT: Time-over-threshold

Closer look on the ToT profile:

- Where do the maxima at the boundaries originate from?

  → Expectation: ToT is constant beyond the boundaries as charge is deposited at the maximum positions

  → The maxima originate from the assumption that the focal point positions aligns with the position of the dominant contribution to the current transient

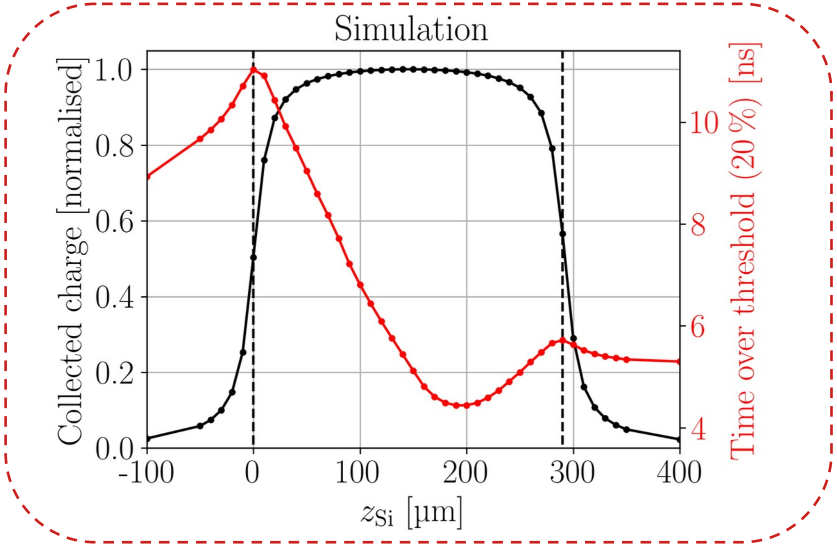

Plots from S. Pape Thesis (2024)

TPA charge carrier density along depth:

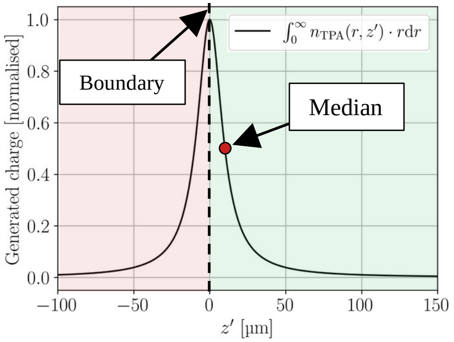

The median is central when the full distribution is inside the active volume, **but the median position shifts when one is close to the boundaries.**

This causes the ToT to become "symmetric" around the boundaries!

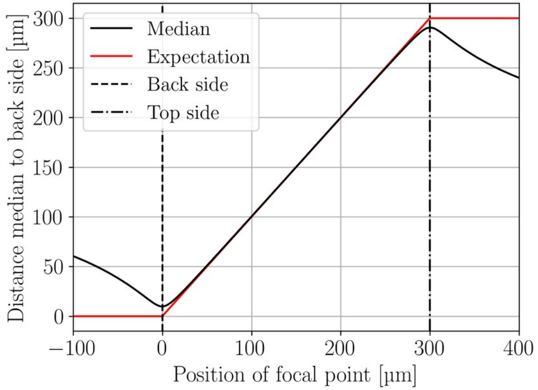

TCAD simulation of TPA-TCT: Weighted prompt current

Closer look on the WPC profile:

1) Where do the valleys at the boundaries originate from?

→ Expectation: E-Field of PIN is linear and is maximal at the top side

→ Depth of valleys increases with the t_{pc}

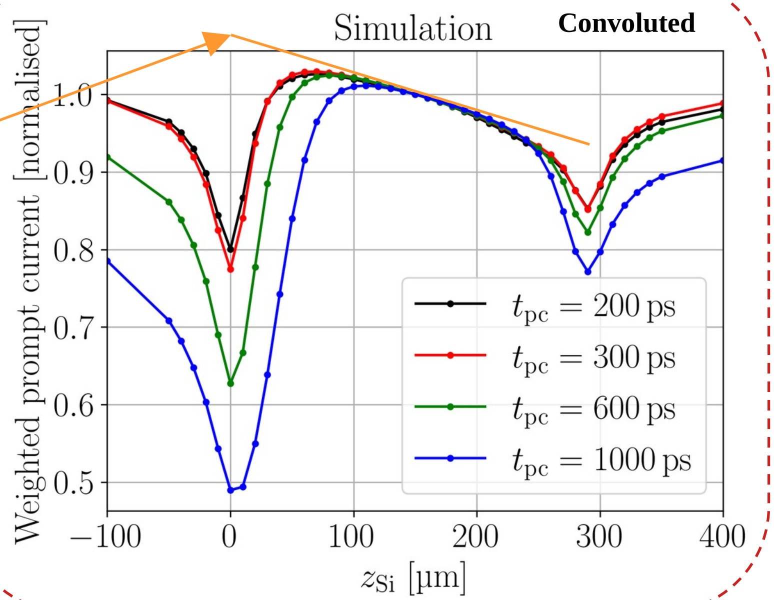

Plots from S. Pape Thesis (2024)

TCAD simulation of TPA-TCT: Weighted prompt current

Closer look on the WPC profile:

1) Where do the valleys at the boundaries originate from?

→ Expectation: E-Field of PIN is linear and is maximal at the top side

→ Depth of valleys increases with the t_{pc}

→ It is not an effect of the readout electronics as it also appears in the non-convoluted WPC

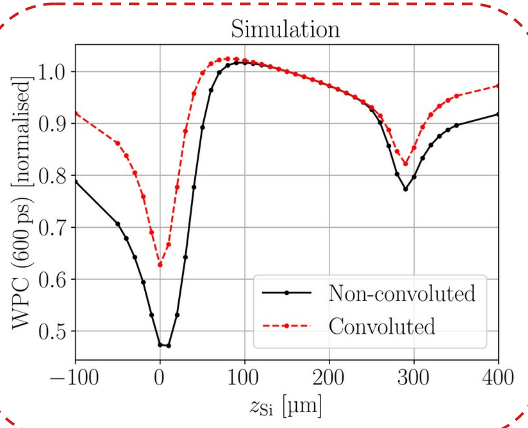

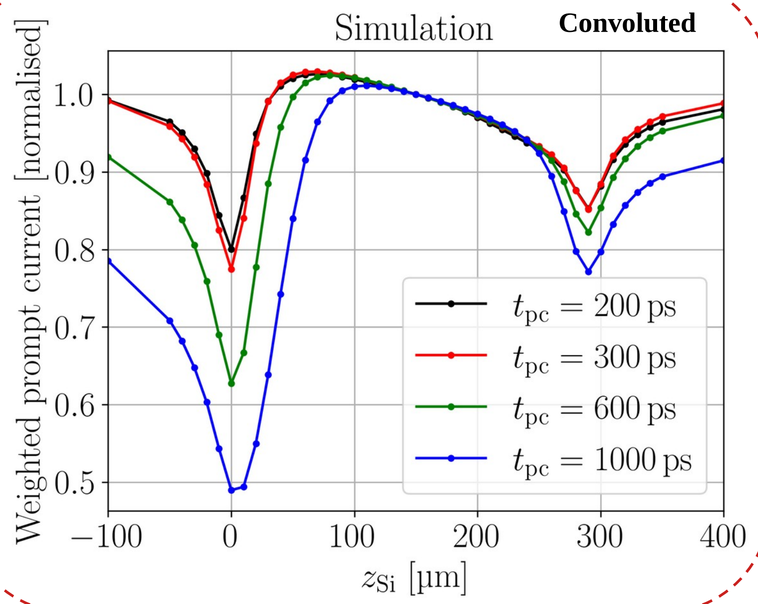

Plots from S. Pape Thesis (2024)

TCAD simulation of TPA-TCT: Weighted prompt current

Closer look on the WPC profile:

1) Where do the valleys at the boundaries originate from?

→ Expectation: E-Field of PIN is linear and is maximal at the top side

→ Depth of valleys increases with the t_{pc}

→ It is not an effect of the readout electronics as it also appears in the non-convoluted WPC

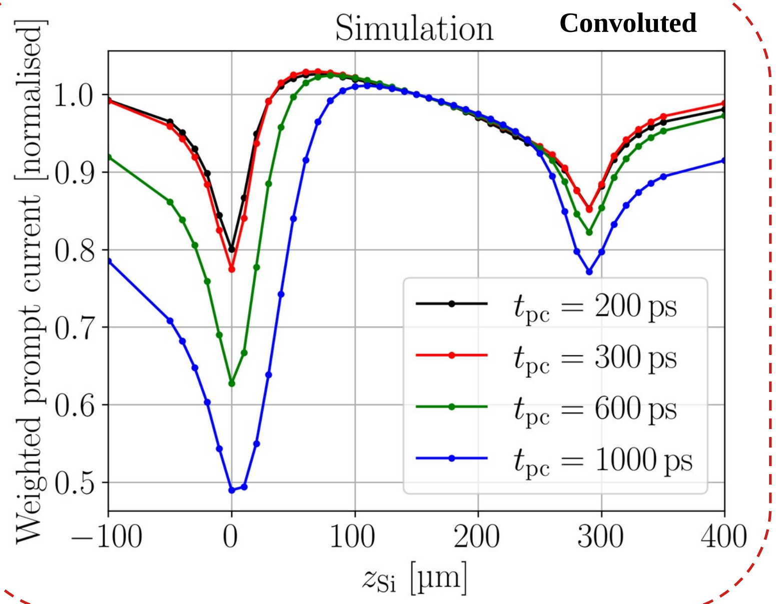

Plots from S. Pape Thesis (2024)

1) Valleys are related charge collection during t_{pc} → not all the injected carriers contribute to the transient current at t_{pc} → lower prompt current

TCAD simulation of TPA-TCT: Weighted prompt current

Closer look on the WPC profile:

1) Where do the valleys at the boundaries originate from?

   → Expectation: E-Field of PIN is linear and is maximal at the top side

   → Depth of valleys increases with the t_{pc}

   → It is not an effect of the readout electronics as it also appears in the non-convoluted WPC

2) Where does the symmetry around the boundaries comes from?

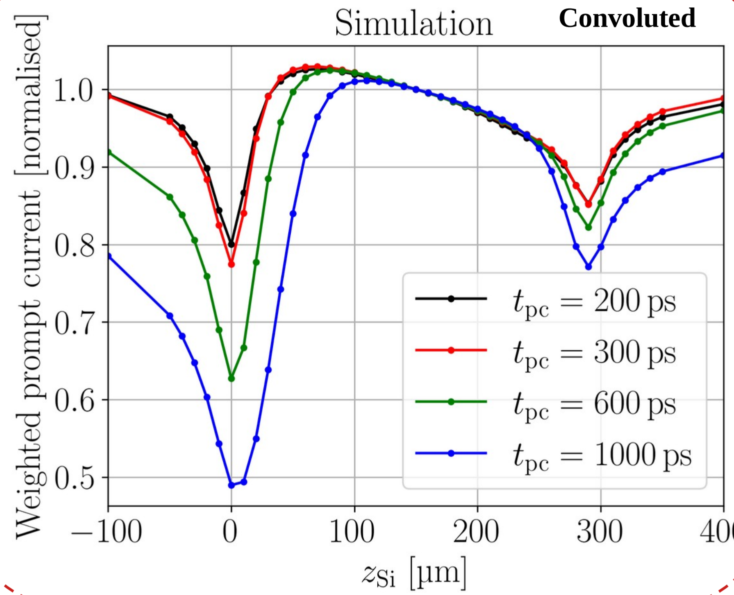

Plots from S. Pape Thesis (2024)

---

1) Valleys are related charge collection during t_{pc} → not all the injected carriers contribute to the transient current at t_{pc} → lower prompt current

TCAD simulation of TPA-TCT: Weighted prompt current

Closer look on the WPC profile:

1) Where do the valleys at the boundaries originate from?

   → Expectation: E-Field of PIN is linear and is maximal at the top side

   → Depth of valleys increases with the t_{pc}

   → It is not an effect of the readout electronics as it also appears in the non-convoluted WPC

2) Where does the symmetry around the boundaries comes from?

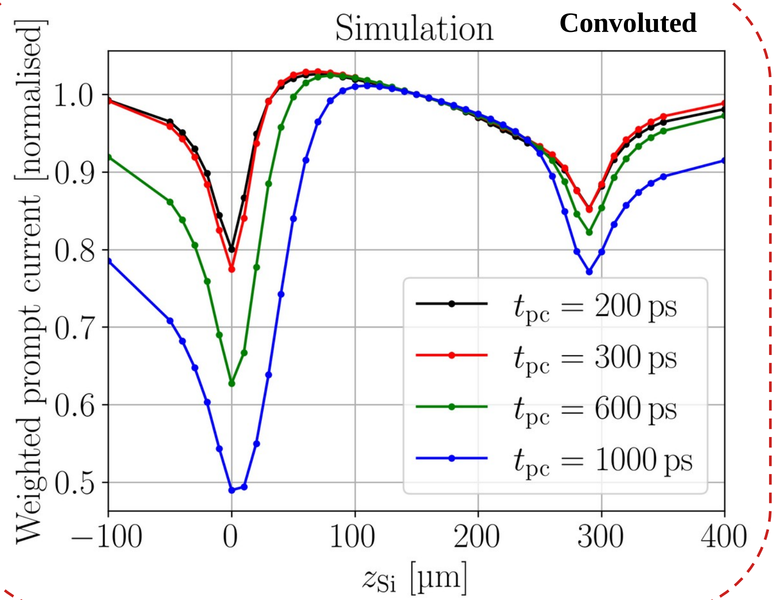

Plots from S. Pape Thesis (2024)

---

1) Valleys are related charge collection during t_{pc} → not all the injected carriers contribute to the transient current at t_{pc} → lower prompt current

2) Same argument as for the symmetry in the ToT → median of the excess charge distribution shifts at boundaries

Part II

Influence of Radiation Damage on the TPA-TCT

Details about the used samples

Design of the planar sensors:

CiS Forschungsinstitut für Mikrosensorik GmbH

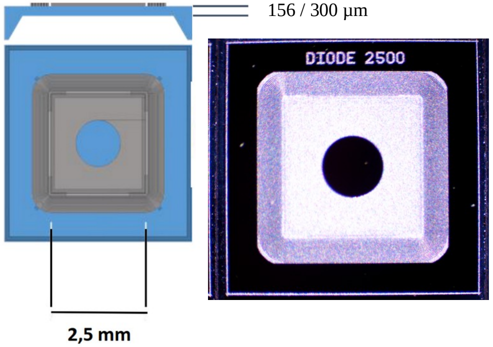

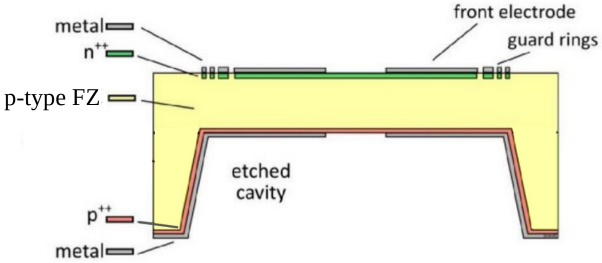

CiS16 FZ planar diodes, p-type, >10kΩ·cm, 2.632×2.632mm^2 active area

Thickness [µm]	Type of irradiation	Facility	Fluence	Annealing
300	Neutron	TRIGA JSI	≤ 7.02×10^{15} n / cm2	10 min @ 60°C 6600 min @ 20 °C
156	Neutron	TRIGA JSI	≤ 7.02×10^{15} n / cm2	10 min @ 60 °C 6600 min @ 20 °C
156	Proton	CERN PS (23GeV)	≤ 1.17×10^{16} p / cm2	10 min @ 60 °C 6600 min @ 20 °C
156	Gamma	IRB Zagreb (^{60}Co)	< 200 Mrad	None

Measurement temperature: (-20±0.1) °C
Humidity: flushed with dry air (~0%)

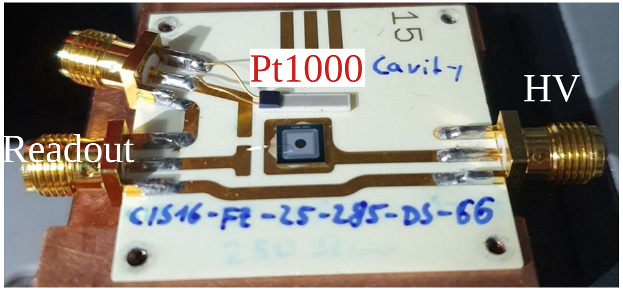

Influence of radiation damage on the TPA-TCT

→ Radiation damage can introduce new energy levels in the band gap that trap charge carriers

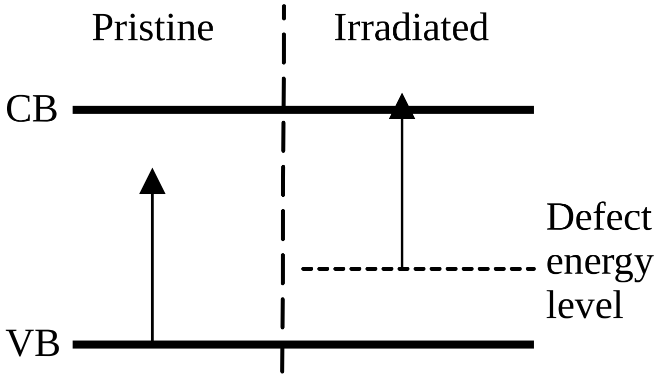

→ Trapped charge carriers can be excited by a single 1550 nm photon

→ This enables a parasitic single photon absorption component to the TPA-TCT measurement

In depth measurements of neutron irradiated PINs:

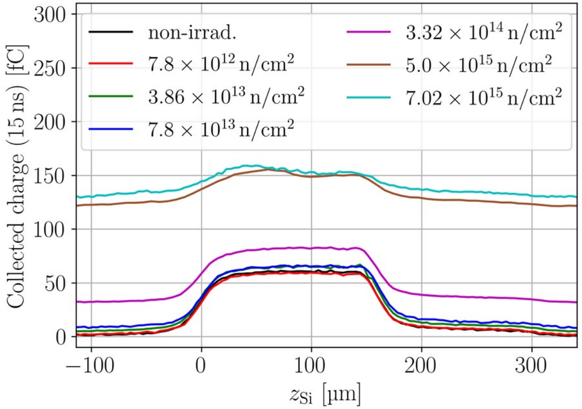

Plots from S. Pape Thesis (2024)

→ Additional SPA component is found as a offset, as it is not depth dependent $Q_{\mathrm{SPA}}(z) = \mathrm{const}$

→ Different methods to correct this SPA component were developed

Comparison between neutron, proton, and gamma irradiated samples

In-depth scans:

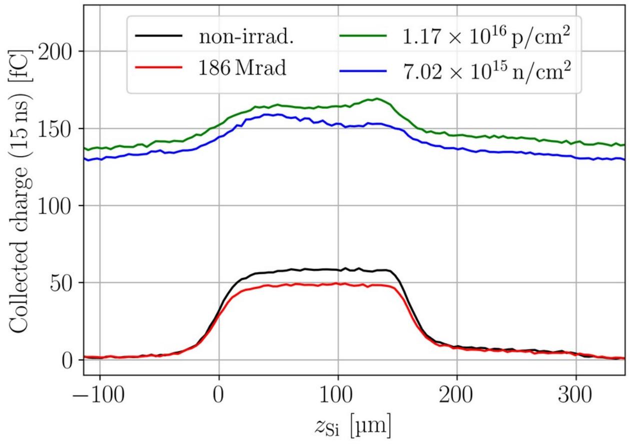

In-depth scans (SPA corrected):

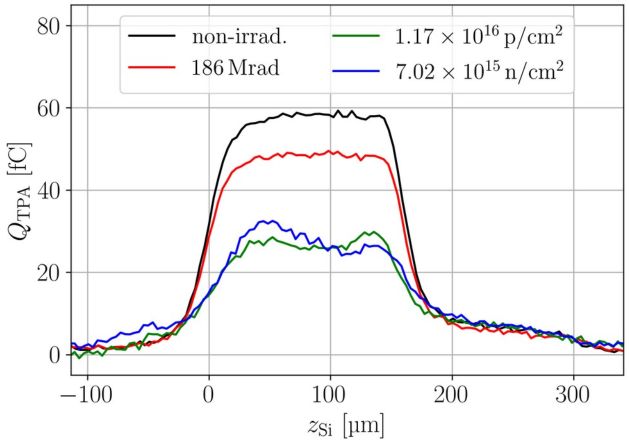

Plots from S. Pape Thesis (2024)

Neutron & proton irradiation:

→ Both lead to a SPA offset
→ Charge loss depends on depth position of charge deposition
→ for the picked fluence they both show a double junction (see prompt current plots in the backup)

Gamma irradiation:

→ **No SPA offset visible!**
→ Charge loss is constant throughout the device depth

Neutron & Proton irradiated PIN: Prompt current profiles

Plots from S. Pape Thesis (2024)

Neutron irradiation 7.02·10^{15} n/cm^2:

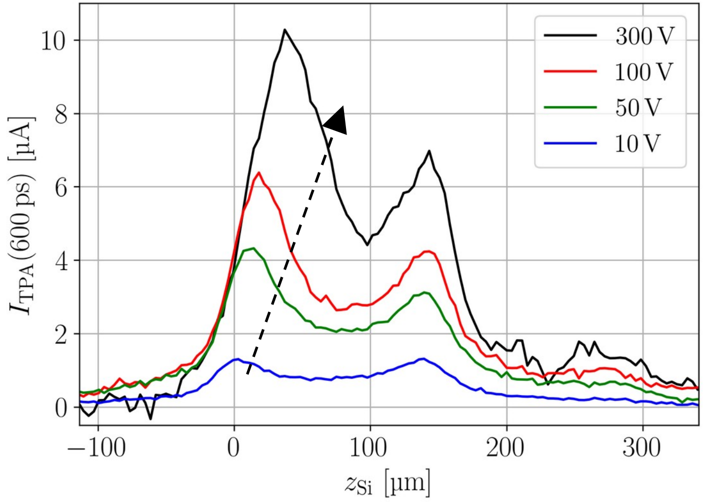

23 GeV proton irradiation 1.17·10^{16} p/cm^2 ($\Phi_{eq} \approx$ 7.25·10^{15}/cm^2):

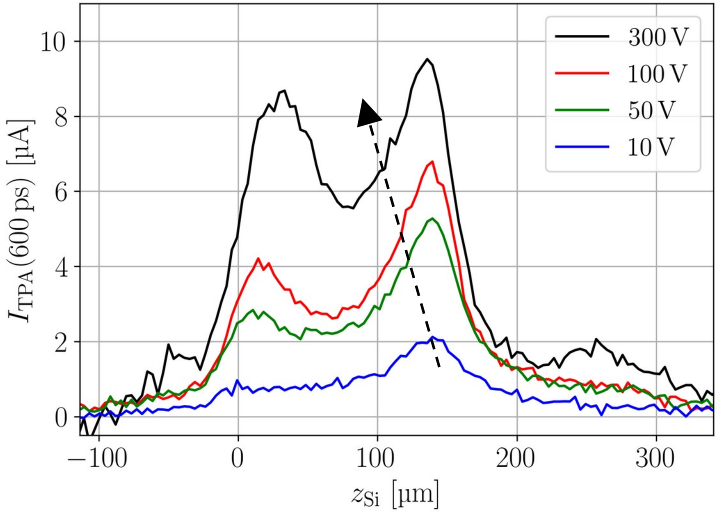

→ Both detectors show a double junction, but the maximum of electric field and growth direction appears on opposite sites

Neutron & Proton irradiated PIN: Prompt current profiles

Neutron irradiation $7.02 \cdot 10^{15}$ n/cm²:

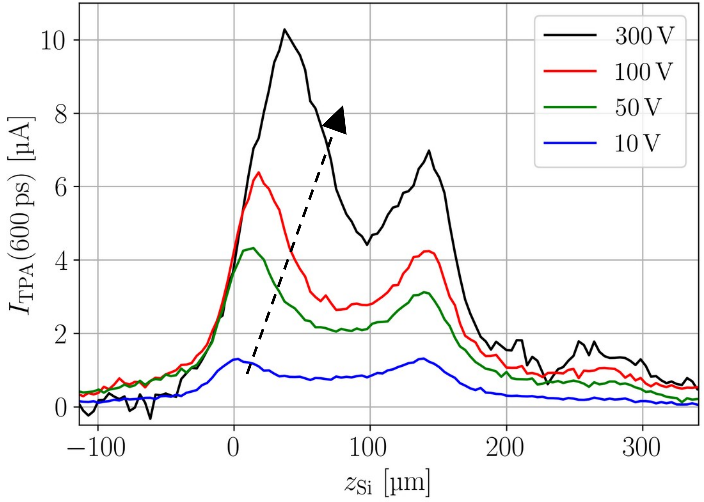

23 GeV proton irradiation $1.17 \cdot 10^{16}$ p/cm² ($\Phi_{eq} \approx 7.25 \cdot 10^{15}$/cm²):

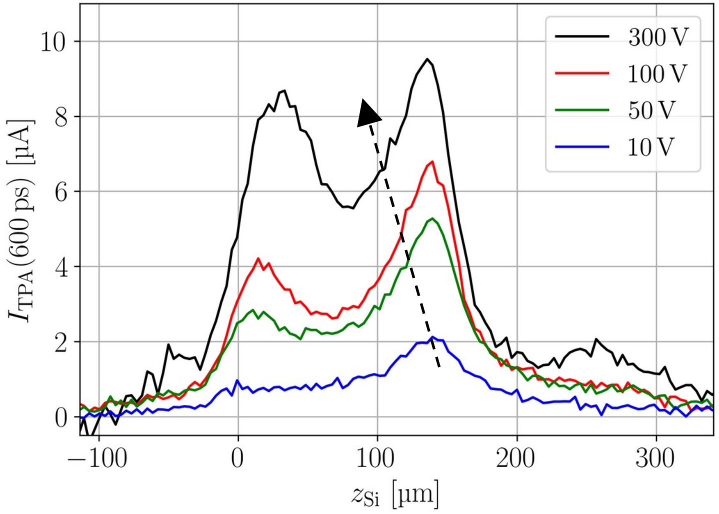

Plots from S. Pape Thesis (2024)

→ Both detectors show a double junction, but the maximum of electric field and growth direction appears on opposite sites
→ Proton irradiated device appears inverted compared to the neutron irradiated one.
→ "Space charge sign inversion" in FZ p-type at high proton irradiation!

Influence of irradiation on the linear absorption coefficient α

Irradiation changes the linear absorption [Fan et al., Fretwurst et al.].
→ The absorption coefficient is linked to the amount of generated charge and measured by the collected charge:

$$\alpha_{\mathrm{eff}} = -\frac{1}{d} \ln \left(1 - Q_{\mathrm{SPA}} \frac{\hbar\omega}{eE_{\mathrm{p}}} \right)$$

Q_{SPA}: charge only generated by linear absorption
d: device thickness

If all charge is collected, $\alpha_{eff} = \alpha_{irr}$ as defined by Fretwurst et al.

Influence of irradiation on the linear absorption coefficient α

Irradiation changes the linear absorption [Fan et al., Fretwurst et al.].
→ The absorption coefficient is linked to the amount of generated charge and measured by the collected charge:

$$\alpha_{\text{eff}} = -\frac{1}{d} \ln\left(1 - Q_{\text{SPA}} \frac{\hbar\omega}{eE_{\text{p}}}\right)$$

Q_{SPA}: charge only generated by linear absorption
d: device thickness

If all charge is collected, $\alpha_{\text{eff}} = \alpha_{\text{irr}}$ as defined by Fretwurst et al.

α_{eff} for different thicknesses and fluences:

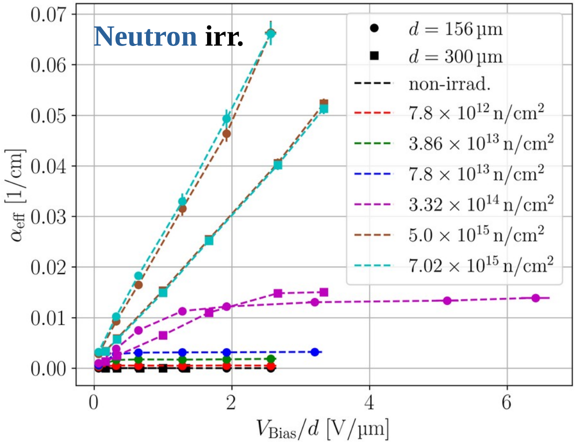

- Increasing bias voltages saturate the α_{eff}, when charge loss saturates
- Higher thickness increases the needed voltage to saturate the Q_{SPA}
- Thickness should not influence α_{eff}
- Highest fluences do not saturate Q_{SPA}

Plot from S. Pape Thesis (2024)

Influence of irradiation on the linear absorption coefficient α

Irradiation changes the linear absorption [Fan et al., Fretwurst et al.].
→ The absorption coefficient is linked to the amount of generated charge and measured by the collected charge:

$$\alpha_{\text{eff}} = -\frac{1}{d} \ln\left(1 - Q_{\text{SPA}} \frac{\hbar\omega}{eE_{\text{p}}}\right)$$

Q_{SPA}: charge only generated by linear absorption
d: device thickness

If all charge is collected, $\alpha_{eff} = \alpha_{irr}$ as defined by Fretwurst et al.

α_{eff} for different thicknesses and fluences:

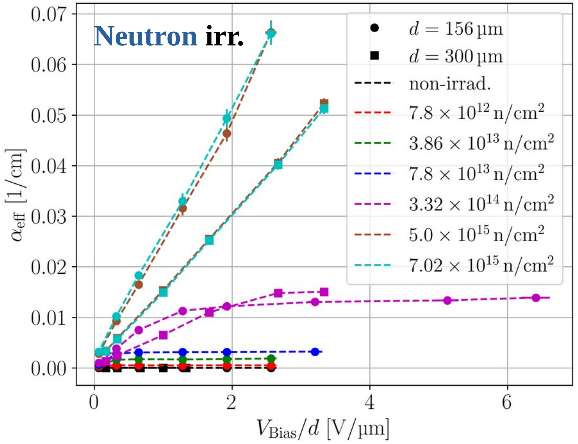

- Increasing bias voltages saturate the α_{eff}, when charge loss saturates
- Higher thickness increases the needed voltage to saturate the Q_{SPA}
- Thickness should not influence α_{eff}
- Highest fluences do not saturate Q_{SPA}

- Proton and neutron irradiation leads to similar results → Cluster defect related [Fretwurst et al.]

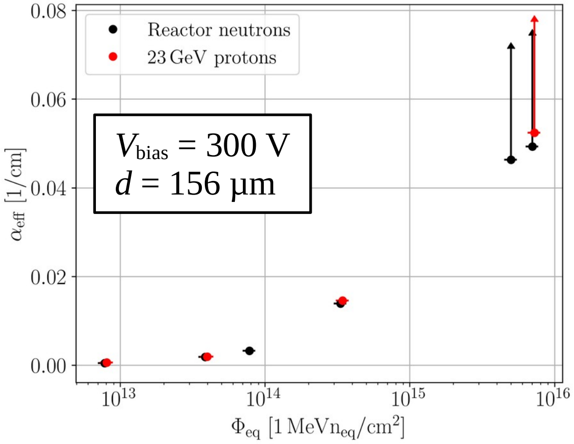

Plots from S. Pape Thesis (2024)

Citations:
H.Y. Fan and A.K. Ramdas - Infrared Absorption and Photoconductivity in Irradiated Silicon

E. Fretwurst et al. - Study of the V_2^0 state in neutron-irradiated silicon using photon-absorption measurements

Influence of irradiation on the refractive index

The laser beam moves different in silicon and air, due to the higher refractive index. The scaling factor $s = z_{\mathrm{Si}}/z$ is related to the refractive index:

$$n^2 = \sqrt{\frac{(\gamma - s^2)^2}{4} + \gamma} - \frac{\gamma - s^2}{2} \, ,$$

with $\gamma = (\lambda s^2)/(\pi z_{\mathrm{R}})$.

Influence of irradiation on the refractive index

The laser beam moves different in silicon and air, due to the higher refractive index. The scaling factor $s = z_{\mathrm{Si}}/z$ is related to the refractive index:

$$n^2 = \sqrt{\frac{(\gamma - s^2)^2}{4} + \gamma} - \frac{\gamma - s^2}{2} \, ,$$

with $\gamma = (\lambda s^2)/(\pi z_{\mathrm{R}})$.

Extracting the device thickness and comparing them to the non-irrad. device allows to calculate the change in the refractive index.

Changes in n for fluences up to $\Phi_{eq} = 3.32 \cdot 10^{14}/\mathrm{cm}^2$ and doses up to 186 Mrad are at least < 5.5 %.

Uncertainty in the measurements is large, but shows that changes in n are at least not dominant.

Extracted refractive index:

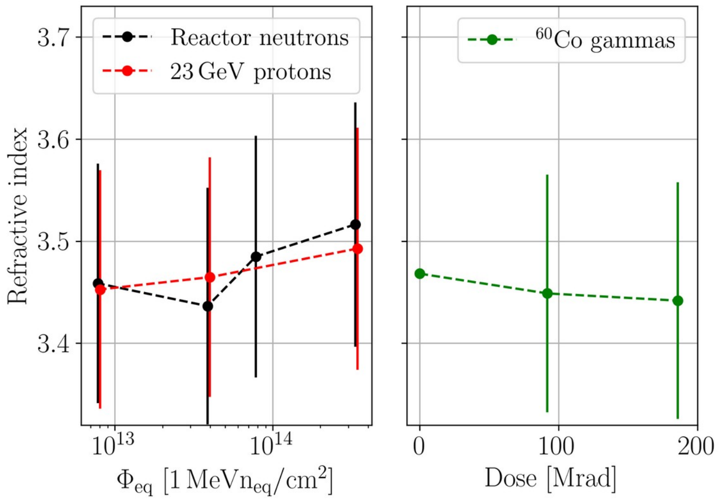

Plot from S. Pape Thesis (2024)

Summary

TCAD

- TPA-TCT measurements can be simulated with TCAD
  → Measurements in a pad detector are well reproduced → all qualitative features found
- Prompt current (PC) and weighted PC have problems at the device boundaries
  → Charge collection during t_{pc} lowers the PC; shorter t_{pc} help to reduce the problems, but are limited by readout electronics

Rad. damage

- Systematic study of influence of radiation damage on the TPA-TCT → n, p, γ irradiation
- "Space charge sign inversion" in proton irradiated FZ p-type ($\Phi_{eq} \approx 7.25 \cdot 10^{15}/cm^2$)
- Effective linear absorption coefficient similar at same Φ_{eq} for neutron and proton irrad. devices
  → Cluster damage related
- Medium fluences/doses ($\Phi_{eq} = 3.32 \cdot 10^{14}/cm^2$ and 186 Mrad) do not significantly change the refractive index n

Thank you!

RD50 2002 - 2023

This work has received funding from the European Union's Horizon 2020 Research and Innovation programme under GA no 101004761 (AIDAinnova) and the Wolfgang Gentner Programme of the German Federal Ministry of Education and Research (grant no. 13E18CHA).

Federal Ministry of Education and Research

BACKUP

TPA-TCT: Setup & Calibration

Sketch of the TPA-TCT setup at CERN SSD:

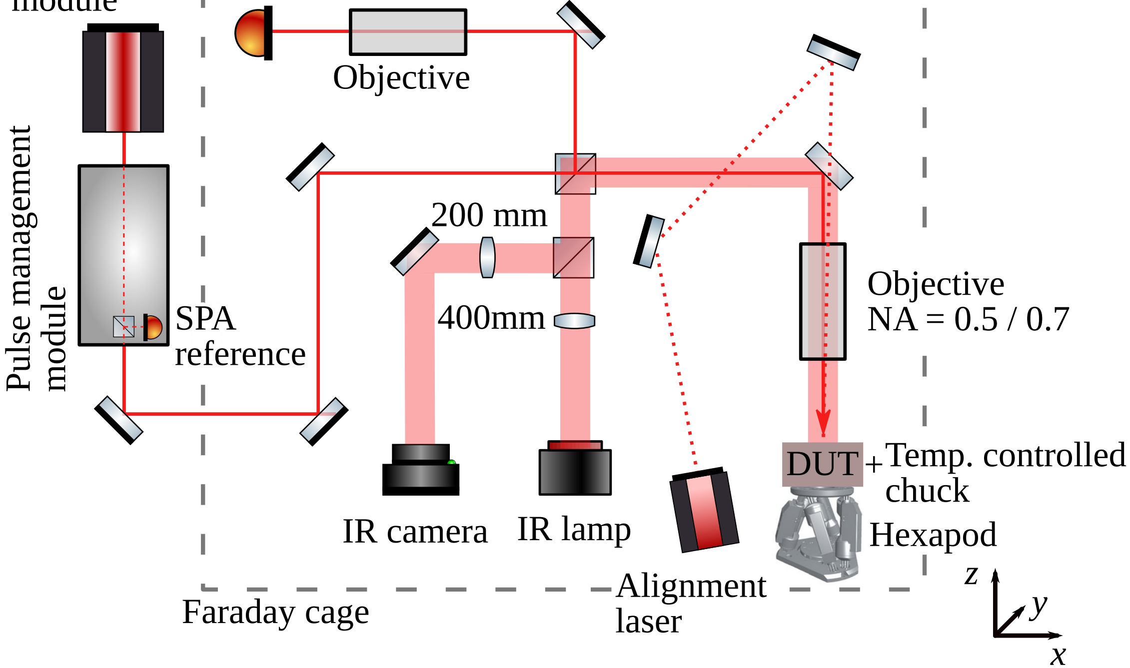

Calibration:

Pulse energy against generated charge (in a 300 µm PIN):

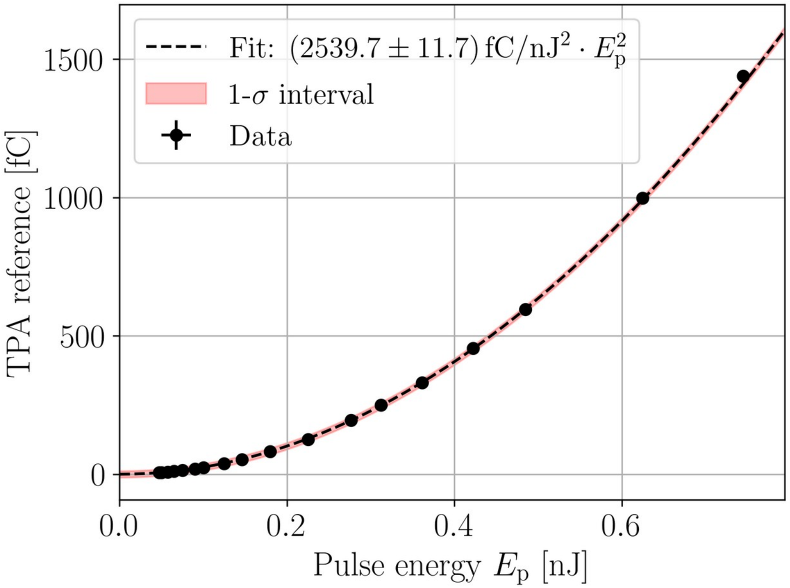

Plot from S. Pape Thesis (2024)

The pulse energy is measured with a S401C thermal power sensor from Thorlabs.

$Q = \cancel{\alpha I} + \beta_2 I^2$ → pure quadratic behavior shows absence of SPA

M. Wiehe et al.:
Development of a Tabletop Setup for the Transient Current Technique Using Two-Photon Absorption in Silicon Particle Detectors

TPA-TCT setup at CERN SSD

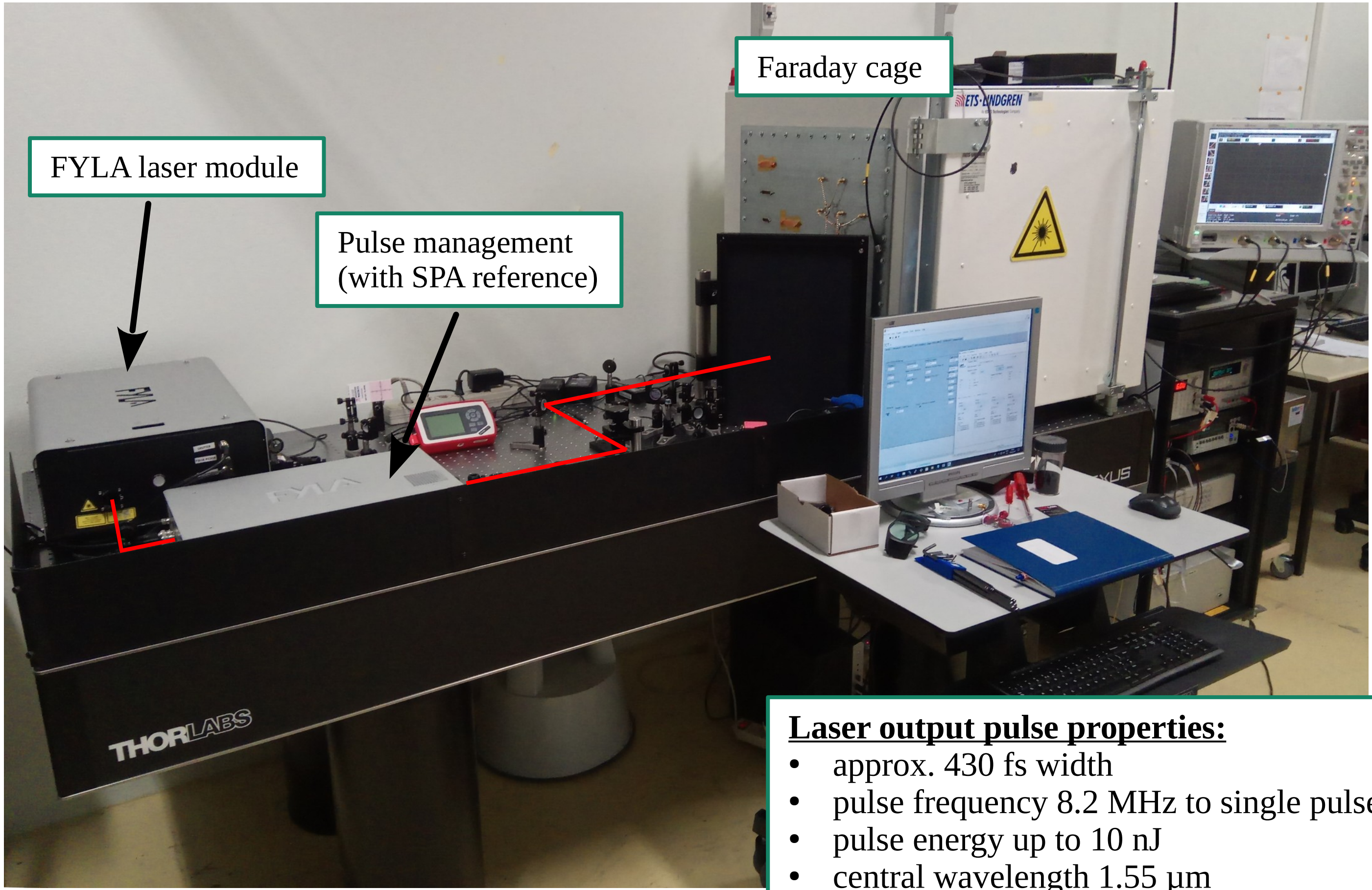

Laser output pulse properties:
- approx. 430 fs width
- pulse frequency 8.2 MHz to single pulse
- pulse energy up to 10 nJ
- central wavelength 1.55 µm

M. Wiehe et al.: *Development of a Tabletop Setup for the Transient Current Technique Using Two-Photon Absorption in Silicon Particle Detectors*

WE LASER THE NEW INDUSTRY

TPA-TCT setup: Inside of the Faraday cage

IR microscope picture of a metal strip: